

## SYSTEMATICS OF $\alpha$ -DECAY HALF-LIVES OF SUPERHEAVY NUCLEI

I. SILIȘTEANU<sup>1</sup>, A.I. BUDACA<sup>2</sup>

<sup>1,2</sup>Department of Theoretical Physics,  
Horia Hulubei National Institute for R&D in Physics and Nuclear Engineering,  
30 Reactorului St., Magurele, jud. Ilfov, P.O.B. MG-6, RO-077125, Romania,  
*E-mail*<sup>1</sup>: silist@theory.nipne.ro  
*E-mail*<sup>2</sup>: abudaca@theory.nipne.ro

Received July 29, 2013

*Abstract.* A brief summary of the calculated and experimental ground state-ground state  $\alpha$ -half-lives of the superheavy nuclei with  $Z=102-120$  is presented. The shell model rate theory is used to calculate  $\alpha$ -decay half-lives in terms of the clustering and scattering amplitudes. Special attention is given to the shell structure and the resonance scattering effects in the decay channel. Theoretical results are confronted to data and other relevant estimates. First systematics of  $\alpha$ -decay properties of SHN was performed by studying the half-life *vs.* energy correlations in terms of atomic number and mass number. Such a systematics shows that the transitions between even-even nuclei are favored, while all other transitions with odd nucleons are prohibited. The accuracy of theoretical calculations is discussed

*Key words:* Super-heavy nuclei (SHN);  $\alpha$ -decay;  $\alpha$ -decay systematics.

*PACS:* 25.70.Jj; 27.90.+b

### 1. INTRODUCTION

The last few years brought impressive progress in synthesizing and studying properties of superheavy nuclei (SHN). Both the amount and quality of experimental data on the nuclear energy levels and decay modes of SHN have increased tremendously [1–15]. The review [16] gives a brief historical overview of the discovery of SHN, the present status and the possibilities for future discoveries.

Among the fundamental properties of SHN the ones which should be established first are possible radioactive decay modes, partial half-lives, and their relative probabilities. The data reveal that the dominant decay modes for the SHN is  $\alpha$ -emission, not fission. There are several efforts to correlate existing  $\alpha$ -decay data on empirical basis in order to give insight into the nature of the process. However, on this way is difficult to correlate data with the evolutions of nuclear structure observ-

ables. The main features of the nuclear structure can be revealed by observing the evolution of some basic quantities that characterize the nucleus [17].

Detailed  $\alpha$ -decay studies [18–23] provide the access to the basic properties of SHN: masses, energy levels, lifetimes, spins, moments, reaction energies and emission rates. Moreover,  $\alpha$ -decay has become a powerful tool to explore the nuclear structure (fine structure, shell effects,  $\alpha$  clustering and deformation) and also of the most important aspects of reaction mechanisms (resonance tunneling, phase transitions and channel coupling).  $\alpha$ -decay of SHN has yielded much energy level information for nuclear spectroscopy and it is one of the most useful probes for studying the structure of the SHN [24]. Detailed experimental and theoretical studies of SHN are revealing new competing decay modes and complex nuclear structures involving weakly bound states coupled to an environment of scattering states.

The knowledge of properties of these nuclei helps to elaborate and improve theoretical models which may be used to predict radioactive properties of unknown species. Such predictions can be made with a fair degree of confidence and this may help in the preparation and identification of new SHN.

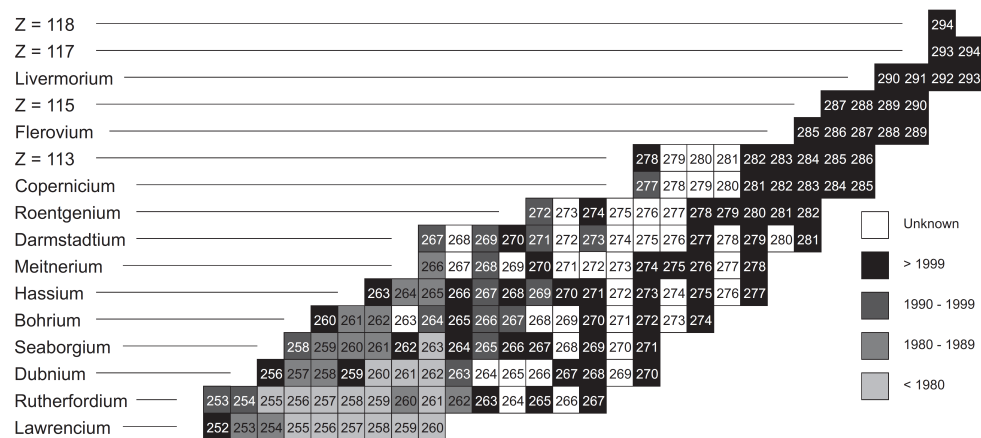


Fig. 1 – Chart of nuclides for elements heavier than nobelium. The grey-scale coding refers to the decade of discovery. This figure is taken from ref. [16]

## 2. SHELL MODEL RATE THEORY

The approach used here to describe the  $\alpha$ -decay process is presented in [23,24]. The procedure is to match smoothly [25] the shell model (SM) wave functions of four individual nucleons ( $I_n^{k[SM]}(r)$ ) with the outgoing  $\alpha$ -particle wave function (from the resonance state  $k$  in channel  $n$ ) which is a general solution of the system of

differential equations:

$$\left[ \frac{\hbar^2}{2m} \left( \frac{d^2}{dr^2} - \frac{l(l+1)}{r^2} \right) - V_{nn}(r) + Q_n \right] u_n^0(r) + \sum_{m \neq n} V_{nm}(r) u_m^0(r) = 0, \quad (1)$$

$$\left[ \frac{\hbar^2}{2m} \left( \frac{d^2}{dr^2} - \frac{l(l+1)}{r^2} \right) - V_{nn}(r) + Q_n \right] u_n^k(r) + \sum_{m \neq n} V_{nm}(r) u_m^k(r) = I_n^{k[SM]}(r). \quad (2)$$

These equations define an  $\alpha$ -particle of given kinetic energy  $Q_\alpha$  and angular momentum  $l$  moving in the potential  $V_{nm}(r)$ . The solutions of the above system represent the radial motion of the fragments at large and small separations, respectively, in terms of the reduced mass of the system  $m$ , the kinetic energy of emitted particle  $Q_\alpha = Q_n = E - E_D - E_\alpha$ , the FA  $I_n^k(r)$ , and the matrix elements of interaction potential  $V_{nm}(r)$ .

The effective decay energy used in the above relations is

$$Q_\alpha = \frac{A}{A-4} E_\alpha^{exp} + \left( 6.53 Z_d^{7/5} - 8.0 Z_d^{2/5} \right) 10^{-5} \quad (3)$$

where,  $A$  is the mass number of the parent nucleus,  $E_\alpha^{exp}$  is the measured kinetic energy of  $\alpha$ -particle, and the second term is the screening correction [26].

The matrix elements  $V_{nm}(r)$  include nuclear and Coulomb components [27] defined with the quadrupole ( $\beta_2$ ) and hexadecapole ( $\beta_4$ ) deformation parameters of the daughter nucleus. To avoid the usual ambiguities encountered in formulating the potential for the resonance tunneling of the barrier we iterate directly the nuclear potential in the equations of motion [27, 28].

The SM  $\alpha$ -particle formation amplitude (FA) is defined as the antisymmetrized projection of the parent wave function on the channel wave function:

$$I_n^{k[SM]}(r) = r \langle \Psi_k^{SM}(r_i) | \mathcal{A} \{ [\Phi_D^{SM}(\eta_1) \Phi_p(\eta_2) Y_{lm}(\hat{r})]_n \} \rangle, \quad (4)$$

where  $\Phi_D^{SM}(\eta_1)$  and  $\Phi_\alpha(\eta_2)$  are the internal (space-spin) wave functions of the daughter nucleus and of the particle,  $Y_{lm}(\hat{r})$  is the wave function of the angular motion,  $\mathcal{A}$  is the inter-fragment antisymmetrizer,  $r$  connects the centers of mass of the fragments, and the symbol  $\langle | \rangle$  means integration over the internal coordinates and angular coordinates of relative motion.

The shell model overlap integral (Eq.4) is estimated for the harmonic oscillator single particle wave functions of the parent and daughter nuclei by using the numerical codes based on analytical formulas [23] (for the passing from individual coordinates  $r_i$  to the center of mass  $r$ , and  $\rho_1 \rho_2 \rho_3$  coordinates). For nuclei with  $Z = 102 - 120$  we use single proton states [29]:  $1i_{13/2}, 2f_{7/2}, 2f_{5/2}, 3p_{3/2}, 3p_{1/2}$ ; and

for nuclei with  $N = 150 - 178$  single neutron states:  $2g_{9/2}, 2g_{7/2}, 3d_{5/2}, 3d_{3/2}, 4s_{1/2}$ . Fig.2 shows an example of the shell model overlap integral which is dependent on the angular momentum of the  $\alpha$ -particle emitted.

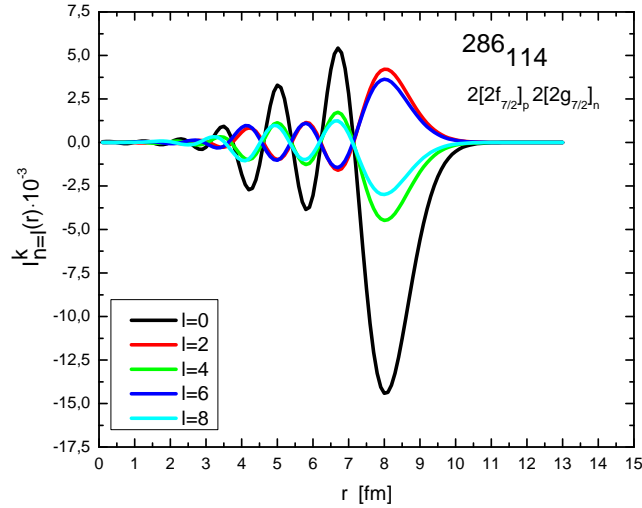


Fig. 2 – The overlap integral computed with harmonic oscillator wave functions for the s.p. configurations  $(2[2f_{7/2}]_p, 2[2g_{7/2}]_n)$  in function of the c.m. distance between the  $\alpha$ -particle and daughter nucleus.

The  $\alpha$ -decay width is given by:

$$\Gamma_n^{k[SM]} = 2\pi \left| \frac{\int_{r_{min}}^{r_{max}} I_n^{k[SM]}(r) u_n^0(r) dr}{\int_{r_{min}}^{r_{max}} I_n^k(r) u_n^{k[SM]}(r) dr} \right|^2, \quad (5)$$

where the lower limit in the integrals is an arbitrary small radius  $r_{min} > 0$ , while the upper limit  $r_{max}$  is close to the first exterior node of  $u_n^0(r)$ .

The  $\alpha$  half-life is expressed as:

$$T_n^{k[SM]} = \ln 2 \cdot \frac{\hbar}{\Gamma_n^{k[SM]}} \quad (6)$$

The  $\alpha$  half-lives derived from Eqs.(6)-(7) depend on the nuclear single particle wave functions and finite sizes of nucleons and  $\alpha$  particles. Also these half-lives include the corrections terms due to screening and resonance scattering effects(see for details [25]).

Finally, the  $\alpha$  half-life should be corrected by even-odd terms  $h_{e-o}$  extracted

from the available decay data.

$$\log T_n^{k[SM]}(s) \implies \log T_n^{k[SM]}(s) + h_{e-o} \quad (7)$$

## 2.1. SYSTEMATICS OF $\alpha$ HALF-LIVES

Interest in the systematics of decay properties starts with the first observations [30] and studies [31] of the natural radioactivity, when it becomes clear that there exists a relationship between the half-life and  $\alpha$ -energy. Thus, the  $\alpha$ -decay properties have been correlated in terms of a few parameters [32,34] which are determined from the fit of decay data. Presently, we compare the systematics of experimental and calculated  $\alpha$ -half lives in order to see the accuracy of the calculations in describing the  $\alpha$ -decay data.

In Fig.3 are plotted the data for (e-e), (e-o), (o-e) and (o-o) nuclei relating the  $\alpha$  half-life and energy ( $\log T_\alpha$  and  $Z_d^{0.6} Q_\alpha^{-1/2}$ ) in which lines of a given parity ( $Z, N$ ) are shown. With a few minor irregularities the experimental half-lives fall on a series of four distinct lines which are near parallel. Fig.3 presents an important distinction between the (e-e) - line (1) and (o-o) - line (4) nuclei, namely the half lives of the later nuclei are significantly larger than the first ones. The lines (2) and (3) corresponding to (e-o) and (o-e) nuclei which are very close to each other are situated in between the lines (1) and (4). The nuclei with odd nucleons show long half-lives as compared with the (e-e) nuclei. The large *rms* values observed in Fig.3 denote significant errors in the data or a low statistics.

From the calculated results in Figs. 4, 5 and 6 (using the measured emission energies) it seems to be a general rule for  $\alpha$ -decay that  $\alpha$ -transitions from odd nuclei are prohibited in comparison with the ones from even nuclei. It is important to note that the general trend of the data with  $Z_d^{0.6} Q_\alpha^{-1/2}$  is well reproduced by the calculated results using the SM rate theory (Fig.4) and empirical results (Figs. 5 and 6) obtained from Eqs. (8) and (9). Again, these calculations show that the  $\alpha$ -decay involving unpaired nucleons ( $Z, N$ )=(e-o,o-e,o-o) proceeds more slowly than that of paired nucleons ( $Z, N$ )=(e-e). The straight lines which correspond to different model approximations in Figs.4-6 are parallel and this fact denotes a common dynamical behaviour described by different reaction models. In fact, the same dependence of the barrier penetrability on the energy is assumed by these models,  $P \sim Q_\alpha^{-1/2}$ .

We prove that the study of  $\alpha$ -decay properties of the SHN in terms of mass number  $A$  and atomic number  $Z$  reveals interesting regularities and correlations. Thus, the values  $\log T_\alpha$  plotted vs.  $Q_\alpha^{-1/2}$  fall on straight lines for the isotopes of a given element  $Z$  (Geiger-Nuttall law).

The values  $\log T_\alpha$  plotted vs.  $Z_d^{0.6} Q_\alpha^{-1/2}$  (Brown law) fall now on the four straight lines which correspond to possible four distinct combinations ( $Z, N$ ): (e,e),

(e,o), (o,e), and (o,o). In this plot the all  $\alpha$ -emitters are ordered in respect with the parity of the proton and neutron numbers.

If comparing the calculated values of  $\alpha$  half-lives (Figs. 4, 5 and 6) with the experimental ones (Fig.3) the conclusions are summarized as follows:

1. A good agreement between  $T^{SM}$  (Fig.4) and  $T^{exp}$  (Fig.3) is observed especially for emitters situated near the closed shells ( $Z=108$ ,  $N=162$  and  $Z=114$ , and  $N$  approaching 184) [24].
2.  $T^{SM}$  (Fig.4) values are somewhat larger than the  $T^{exp}$ ,  $T^{VS}$  and  $T^B$  values.
3. The fit parameters in Figs.4 and 5 have very close values and similar standard errors.
4. The  $\alpha$ -decay involving unpaired nucleons ( $Z, N$ ) = (e-o, o-e, o-o) always proceeds more slowly than that involving paired nucleons ( $Z, N$ ) = (e-e).

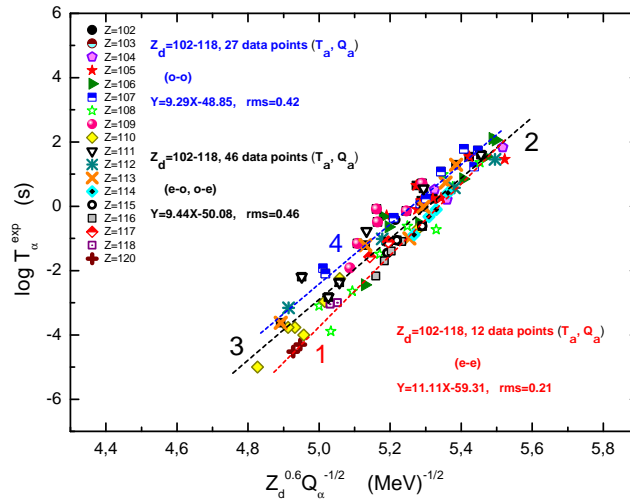


Fig. 3 – The  $\log T_{\alpha}^{exp}$  values [1–15] are plotted vs.  $Z_d^{0.6} Q_{\alpha}^{-1/2}$ . The straight lines represent the best fit to the all known  $\log T_{\alpha}^{exp}$  values for a certain parity ( $Z, N$ ).

Many approaches and methods were employed in theoretical investigation of SHN. Thus, the generalization of the Geiger-Nuttall law has been obtained starting either from the microscopic [35–37] or macroscopic [38] mechanisms of the charged particle radioactivity. The proposed systematics of  $\alpha$ -properties coincides, to a large extent, with our shell model rate systematics.

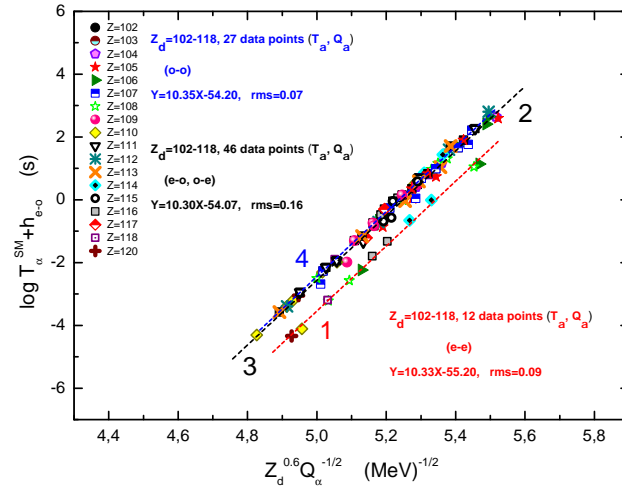


Fig. 4 – The  $\log T_{\alpha}^{SM}$  values calculated with Eq.(7) are plotted vs.  $Z_d^{0.6} Q_{\alpha}^{-1/2}$ . The straight lines represent the linear fit to the all  $\log T_{\alpha}^{SM}$  values corresponding to a certain parity ( $Z, N$ ).

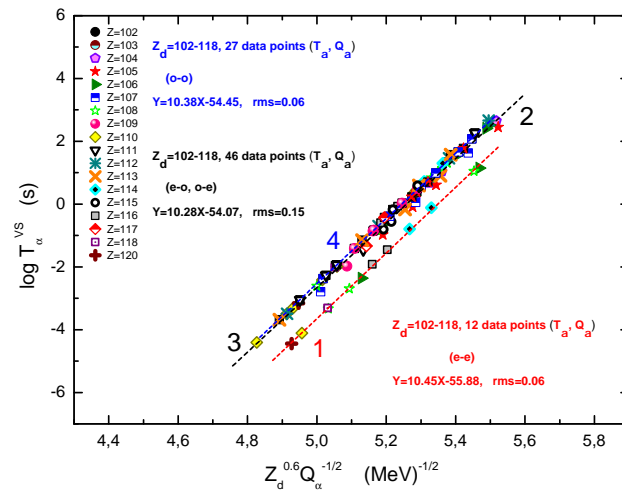


Fig. 5 – The  $\log T_{\alpha}^{VS}$  values calculated with Eq.(8) (which has the even-odd correction  $h_{e-o}$  included) plotted vs.  $Z_d^{0.6} Q_{\alpha}^{-1/2}$ . The straight lines represent the linear fit to the all  $\log T_{\alpha}^{VS}$  values associated to a certain parity ( $Z, N$ ).

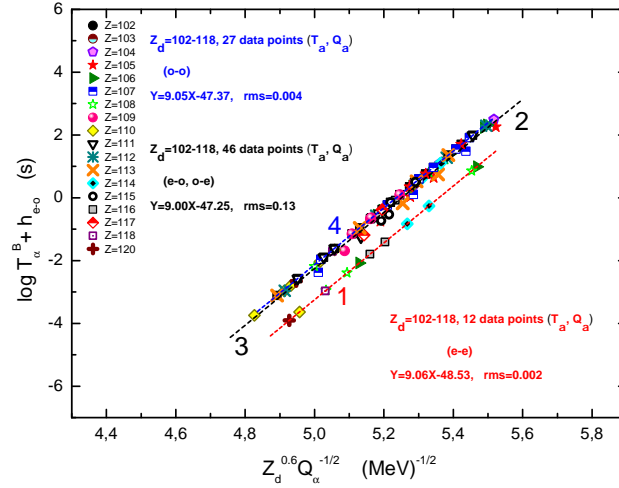


Fig. 6 – The  $\log T_{\alpha}^B$  values calculated with Eq.(9) plus the even-odd correction  $h_{e-o}$  plotted vs.  $Z_d^{0.6} Q_{\alpha}^{-1/2}$ . The straight lines represent the linear fit to the all  $\log T_{\alpha}^B$  values associated to a certain parity ( $Z, N$ ).

These new results in the systematics of decay properties illustrate how the discovery of SHN gives us new nuclear structure information at the limits of stability.

### 3. CONCLUDING REMARKS

Up to now, more than 90 nuclides have been synthesized in spite of the extremely low fusion cross sections. Many nuclear properties of these nuclides have been measured and investigated theoretically. The shell structure is very important for the stability of SHN. This is observed first in the single-particle spectrum where the occurrence of the shells separated by energy gapes. The  $\alpha$ -decay properties appear correlated strongly with the structure of extreme nuclei, but are determined to a large extent, by the assembly of the Fermi nucleons in the  $\alpha$ -particle. The shell model has been shown to be very useful for the understanding the detailed features of  $\alpha$ -decay, such as lifetimes, branching ratios and fine structure.

The systematics of experimental and calculated  $\alpha$  half-lives reveals either some measurement errors, either a lower accuracy of the theory or models, for whose events with a large scatter from the Geiger-Nuttall or Brown laws.

In summary, this work presents a systematization of  $\alpha$ -decay half-lives for all of about 90 observed cases of  $\alpha$ -emitters in SHN. The systematics in two distinct



variants provides a good description of  $\alpha$ -half-lives in the agreement to the data.

#### 4. APPENDIX

Here we consider two phenomenological formulas. The first is the Viola-Seaborg formula [32] which reads as

$$\log T_{\alpha}(s) = (aZ_d + b)Q_{\alpha}^{-1/2} + (cZ_d + d) + h_{e-o} \quad (8)$$

where  $Q_{\alpha}$  is the decay energy in MeV units,  $Z_d$  is the charge number of daughter nucleus;  $a, b, c, d$  are parameters and  $h_{e-o}$  is an even-odd hindrance term. The parameters used are from Ref. [33]:  $a = 1.66175$ ;  $b = -8.5166$ ;  $c = -0.20228$ ;  $d = -33.9069$ ,  $h_{e-e} = 0.0$  ( $Z$ =even,  $N$ =even);  $h_{o-e} = 0.772$  ( $Z$ =odd,  $N$ =even);  $h_{e-o} = 1.066$  ( $Z$ =even,  $N$ =odd);  $h_{o-o} = 1.114$  ( $Z$ =odd,  $N$ =odd).

The second one is the Brown formula [34] written as

$$\log T_{\alpha}(s) = 9.54Z_d^{(0.6)}Q_{\alpha}^{-1/2} - 51.37 + h_{e-o} \quad (9)$$

the constants being determined from the best linear fit of 119 data points ( $T_{\alpha}$ ,  $Q_{\alpha}$ ) in a range of  $Z_d$  from 74 to 106 for even even nuclei.

**Acknowledgements.** We thank to Professors Yu. Ts. Oganessian, V. K. Utyonkov, W. Scheid, A. Săndulescu, M. Mirea, for many stimulating discussions. We are particularly grateful for fruitful discussions with our colleagues from Department of Theoretical Physics, IFIN-HH, Bucharest-Magurele. This work was supported from Contract: Idei **068/05.10.2011**.

#### REFERENCES

1. Y.T. Oganessian *et al.*, Phys. Rev. C **87**, 014302 (2013).
2. Y.T. Oganessian *et al.*, Phys. Rev. C **79**, 024603 (2009).
3. Y.T. Oganessian *et al.*, Phys. Rev. C **76**, 011601(R) (2007).
4. Yu. Oganessian, J. Phys. G **34**, R165 (2007).
5. Y.T. Oganessian, Pure. Appl. Chem. **78**, 889 (2006).
6. S. Hofmann *et al.*, Eur. Phys. J. A **14**, 147 (2002).
7. S. Hofmann, G. Münzenberg, Rev. Mod. Phys. **72**, 733 (2000).
8. S. Hofmann *et al.*, Zeit. Phys. A **354**, 229 (1996).
9. K. Morita *et al.*, Jap. Phys. Soc. J. **73**, 2593 (2004).
10. J. Dvorak *et al.*, Phys. Rev. Lett. **100**, 132503 (2008).
11. P.A. Ellison *et al.*, Phys. Rev. Lett. **105**, 182701 (2010).
12. Ch.E. Düllmann *et al.*, Phys. Rev. Lett. **104**, 252701 (2010).
13. H. Haba *et al.*, Phys. Rev. C **83**, 034602 (2011).
14. J. Piot *et al.*, Phys. Rev. C **85**, 041301 (2012).
15. I. Dragojevic *et al.* Phys. Rev. C. **79**, 011602(R) (2009).
16. M. Thoennessen, Rep. Prog. Phys. **76**, (2013)056301; arXiv:1304.3267v1 [nucl-ex] 11 Apr 2013.

17. D. Bucurescu and N.V. Zamfir, Phys. Rev. C **87**, 054324 (2013).
18. P. Roy Chowdhury, C. Samanta, D.N. Basu, At. Data Nucl. Data Tab. **94**, 781-806 (2008).
19. V.Y. Denisov, A.A. Khudenko, At. Data Nucl. Data Tab. **95**, (2009) 815-835; Phys. Rev. C **79**, 054614 (2009); Phys. Rev. C **80**, 034603 (2009).
20. K.P. Santhosh, *et al.*, Phys. Rev. C **85**, 034604 (2012); J. Phys. G: Nucl. Part. **38**, 075101 (2011).
21. B.K. Sahu *et al.*, Int. J. Mod. Phys. E **20**, 2217-2228 (2011).
22. D. Ni and Z. Ren, Phys. Rev. C **80**, 051303 (2009); Nucl. Phys. A **828** 348-359 (2009); Ren, Rom. J. Phys. **57**, 407-418 (2012).
23. I. Silişteanu, A.I. Budaca, At. Data Nucl. Data Tab., **98**, (2012); Rom. J. Phys. **57**, 493-505 (2012); I. Silişteanu, A.I. Budaca, A.O. Silişteanu, Rom. J. Phys. **55**, 1088-1110 (2010).
24. A.I. Budaca, I. Silişteanu, Rom. Rep. Phys. **63**, 1147-1166 (2011); A.I. Budaca, I. Silişteanu, J. Phys. Conf. Series **337**, 012022 (2012); A.I. Budaca, I. Silişteanu, J. Phys. Conf. Series **413** 012027 (2013).
25. I. Silişteanu, W. Scheid, A. Săndulescu, Nucl. Phys. A **679**, 317 (2001).
26. J.O. Rasmussen, *Alpha-, Beta- and Gamma-Ray Spectroscopy*, vol. **1**, Kay Siegbahn (ed.) (North-Holland Publishing Company, Amsterdam, 1968, p.701).
27. V. Ledoux, M. Rizea, M. Van Daele, G. Vanden Berghe, I. Silişteanu, J. Comput. App. Math. **228**, 197-211 (2009).
28. I. Silişteanu, W. Scheid, Phys. Rev. C **51**, 2023 (1995).
29. A.T. Kruppa *et al.*, Phys. Rev. C **61**, 034313 (2000).
30. H. Geiger, J.M. Nuttall, Philos. Mag. **22**, 613 (1911).
31. I. Perlman, A. Ghiorso, and G.T. Seaborg, Phys. Rev. **77**, 26(1950).
32. V.E. Viola, G.T. Seaborg, J. Inorg. Nucl. Chem. **28**, 741 (1966).
33. A. Sobiczewski, Z. Patyk, S. Cwiok, Phys. Lett. B **224**, 1 (1989).
34. B. Alex Brown, Phys. Rev. C **46**, 811 (1992).
35. C. Qi, *et al.*, Phys. Rev. C **80**, 044326 (2009).
36. A. Săndulescu, M. Mirea, D.S. Delion, EPL **101**, 62001 (2013).
37. D.S. Delion, "*Theory of Particle and Cluster Emission*" (Springer-Verlag, Berlin, 2010).
38. D.N. Poenaru, R.A. Gherghescu, W. Greiner, Phys. Rev. C **83**, 014601 (2011).